DYNAMIC RESPONSE ANALYSIS FOR A LARGE-SCALE RC GIRDER UNDER A FALLING-WEIGHT IMPACT LOADING

N. Kishi[1], T. Ohno[2], H. Konno[3], and A.Q. Bhatti[1]
[1]*Department of Civil Engineering and Architecture, Muroran Institute of Technology, Muroran 050-8585, Japan; E-mail: kishi@news3.ce.muroran-it.ac.jp*
[2]*Department of Civil Engineering, National Defense Academy, Yokosuka 239-8686, Japan*
[3]*Structural Division, Civil Engineering Research Inst. of Hokkaido, Hiragishi, Toyohira-Ward, Sapporo 062-8602, Japan*

Abstract

In order to establish a rational impact resistant design procedure for prototype reinforced concrete (RC) structures, not only experimental study but also numerical analysis study should be conducted. However, numerical analysis method on impact response analysis for those structures has not been established yet. Here, in order to establish a rational numerical analysis method for prototype RC structures under impact loading, a falling-weight impact test was conducted for prototype RC girder with 8 m clear span. Referring to the experimental response waves, numerical accuracy was investigated varying major parameters. From this study, following results were obtained as: (1) fine mesh should be used near supporting gigues; (2) Drucker–Prager yield criterion should be applied which gives better results than von Mises one; and (3) appropriate system damping constant should be set to $h = 0.015$.

Keywords: prototype RC girder, falling-weight impact test, impact response analysis, LS-DYNA, Drucker–Prager yield criterion

1. Introduction

In Japan, design method concerning infrastructures tends to be shifted from allowable stress design method to performance based design one. Under such a situation, however, impact resistant design for RC structures has been still performed based on the allowable stress design concept. To accomplish the shift of design method for RC structures under impact resistant design, experimental and numerical researches for small-scale members have been conducted (JSCE, 2004; Kishi et al., 2001; Kishi et al., 2002). On the other hand, impact research sub-committee of JSCE in Japan was managed round-robin pre/post analysis, which was conducted to confirm the numerical accuracy and characteristics of the method applied by each institution. From those researches, following conclusions were obtained: (1) from the pre-analysis results, it is too difficult to precisely predict numerically both impact force and reaction force waves obtained from the experimental results; and (2) on the contrary, displacement wave can be better simulated comparing with above two response waves.

In general, a basic concept for designing RC members should be constituted based on the research findings for small-scale members and the applicability should be confirmed conducting large-scale experiments. In the cases of RC structures under shock and impact, however, it is not easy to conduct the experiments because of expenses for preparing of specimens and experimental set-up fittings. On the other hand, numerical simulations for large-scale impact test for RC members may be easily performed by using personal computers because of an advanced development of computer technology. Then, a rational impact resistant design procedure for RC members may be better established by

M. Pandey et al. (eds), Advances in Engineering Structures, Mechanics & Construction, 99–109.

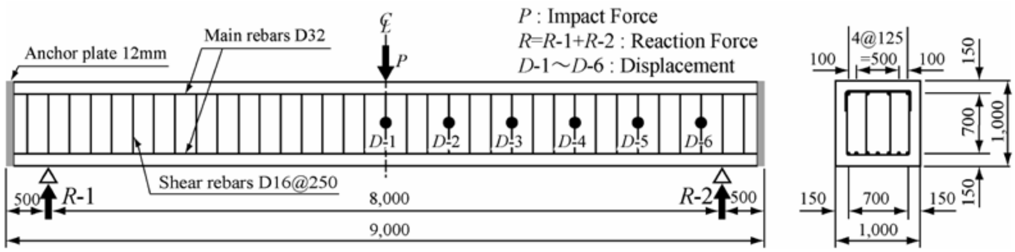

Fig. 1. Dimensions of RC girder and measuring items.

supporting of numerical simulations. To accomplish this, a rational numerical simulation method for large-scale impact test must be established. Authors have discussed numerical simulation method using three-dimensional elasto-plastic finite element technique for small-scale impact test of RC beams (JSCE, 2004; Kishi et al., 1999). However, numerical investigations for large-scale impact tests have not been conducted yet.

From this point of view, in this paper, in order to establish a more precise numerical analysis method for analyzing elasto-plastic impact behavior of prototype RC structures, numerical accuracy of the results obtained using a three-dimensional elasto-plastic finite element method was investigated for each input parameter referring to the experimental results obtained from a falling-weight impact test for large-scale RC girder which was similar to that of designing roof of RC rock-sheds constructed over the highway to ensure people and vehicles safety. In this study, a general-purpose program LS-DYNA code, which is developed based on finite element method is used for those investigations (Hallquist, 2000).

2. Experimental Overview

2.1. *Dimensions and Static Design Values of RC Girder*

In this study, a RC girder, which is for designing roof of real RC rock-sheds, was taken for falling-weight impact test of prototype RC structures. The girder is of rectangular cross section and the dimensions are of 1 m × 1 m and clear span is 8 m long, which is similar to the width of real RC rock-sheds. Figure 1 shows dimensions of the RC girder, distribution of rebar, and measuring points for each response wave. In this figure, it is confirmed that 7#D32 rebars are arranged as main rebar assuming 0.65% of main rebar ratio corresponding to designing of real RC rock-sheds and 4#D32 rebars are arranged as the upper axial rebar to be about a half of main rebar ratio. Thickness of concrete cover is assumed to be 150 mm as well as real rock-sheds. D16 stirrups are arranged with intervals of 250 mm, which is less than a half of an effective height of the girder. In this study, arranging interlayer stirrups and upgrading in shear load-carrying capacity, the RC girder was designed to be collapsed with flexural failure mode. Axial rebars were welded to 12 mm steel-plates at the ends to save the anchoring length of the rebars.

The displacements of the girder were measured at mid-span ($D-1$) and the other five points ($D-2$ to $D-6$) with the intervals of 750 mm from the mid-span. Impact force P was estimated using deceleration of the heavy weight, which is measured using accelerometer set at its top surface. Reaction force R ($= R_1 + R_2$) was also measured using load-cells installed in the supporting gigues. The detailed static design parameters of the RC girder are listed in Table 1. Static flexural and shear load-carrying capacities P_{usc} and V_{usc} were calculated based on Japanese concrete standards (JSCE, 1996). From this table, it is confirmed that the RC girder designed here will collapse with flexural

Table 1. Static design parameters of RC girder.

Shear rebar ratio	Static shear depth ratio	Static shear capacity	Static bending capacity	Shear-bending capacity ratio
ρ_t	a/d	V_{usc} (kN)	P_{usc} (kN)	α
0.0065	4.71	1651	892	1.85

Table 2. Material properties of concrete.

Age (days)	Compressive strength f_c' (MPa)	Young's modulus E_c (GPa)	Poisson's ratio ν_c
36	30.4	27.6	0.186

failure mode under static loading because shear-bending capacity ratio α is larger than unity. The static material properties of concrete and rebars during experiment are listed in Tables 2 and 3, respectively.

2.2. *Experimental Method*

In the experiment, a 2,000 kg heavy weight was lifted up to the prescribed height of 20 m by using the track crane, and then dropped freely to the mid-span of girder with a desorption device. A heavy weight is made from steel outer shell with 1 m in the diameter, 97 cm in height, and spherical bottom with 80 cm in radius as shown in Figure 2(a) and its mass is adjusted filling concrete and steel balls. Figure 2(b) shows supporting gigue including load-cells and Figure 2(c) shows gigue for preventing RC girder from jumping up. RC girder was set on the supporting gigues, which are made so as to freely rotate but not to move toward each other.

The ends of RC girder is fixed in the upward direction using steel rods and beams to prevent from jumping up at the time of impacted by a heavy weight as shown in Figure 2(c). In this experiment, impact force wave (P), reaction force wave (R), and displacement waves (D) at six points along the girder were measured. Impact force wave was estimated using a deceleration of heavy weight, which is measured using accelerometers set at the top-surface of weight.

The accelerometer is of strain gauge type and its capacity and frequency range for measuring are 1,000 times gravity and DC through 7 kHz, respectively. Each load-cell for measuring reaction force are of 1,500 kN capacity and more than 1 kHz measuring frequency. For measuring displacements, laser-type variable displacement transducers (LVDTs) were used which are of 200 mm maximum stroke and 915 Hz measuring frequency. Analog signals from those sensors were amplified and converted to digital ones.

Table 3. Material properties of rebar.

Rebar type	Grade	Yield stress σ_y (MPa)	Young's modulus E_s (GPa)	Poisson's ratio ν_s
D16	SD345	390	206	0.3
D32	SD345	375		

Fig. 2. Pictorial views of heavy weight and supporting gigues.

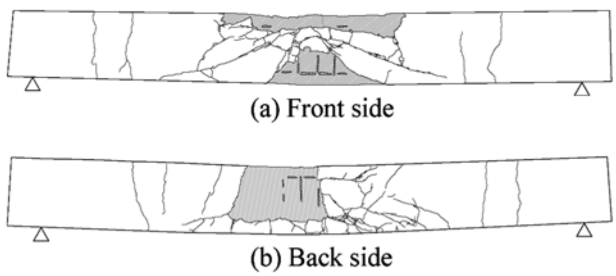

Fig. 3. Crack patterns of RC beam sides after experiment.

The digital data were continuously recorded with 0.1 ms time intervals by using digital data recorders. After that, impact force wave was numerically filtered by means of rectangular moving average method having 0.5 ms time. After experiment, pictures for views of crack patterns occurred around impacted area and on side-surface of RC girder, and a view of peeling and spalling of concrete cover were took. Figure 3 shows crack distributions occurred in the both side-surfaces of the girder.

3. Analytical Overview

3.1. *Finite Element Model*

One quarter of RC girder was three-dimensionally modeled for numerical analysis with respect to the two symmetrical axis. Figure 4(a) shows the mesh geometry of the girder, which is finally used for numerical analysis with an appropriate design accuracy investigated here. A geometrical configuration of heavy weight was modeled as the real one. Supporting gigues including load-cells and gigue for protecting the girder from jumping up were also precisely modeled corresponding to the real ones. In this model, axial rebar and stirrup were modeled using beam element having equivalent axial stiffness, cross sectional area and mass with those of real ones. The other were modeled using eight-node and/or six-node solid elements. The mesh geometries for axial rebar and stirrup are shown in Figure 4(b).

Total number of nodal points and elements for the whole structure shown in Figure 4(a) are 13,963 and 12,360, respectively. Number of integration points for solid and beam elements are one and four, respectively. In order to take into account of contact interface between adjoining concrete and a head of heavy weight elements and between adjoining concrete and supporting gigue elements, contact surface elements for those are defined, in which contact force can be estimated by applying penalty methods for those elements but friction between two contact elements were neglected.

A head of heavy weight was set so as to contact the impacting point of the upper surface of RC girder and predetermined impact velocity was applied to all nodal points of the weight model. The

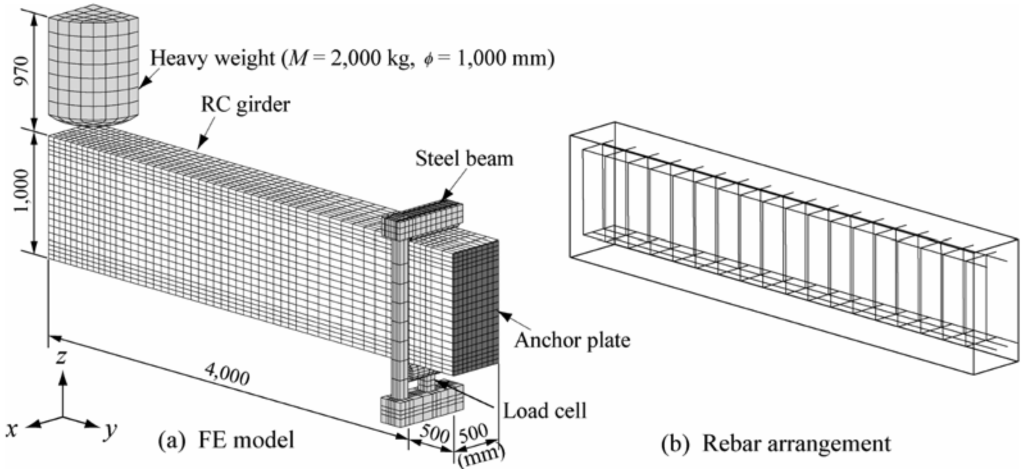

Fig. 4. FE numerical analysis model.

elasto-plastic impact response behavior was analyzed during 400 ms from the beginning of impact to the RC girder reaching steady state. The time increment of numerical analysis has been determined calculating in the LS-DYNA code based on a Courant numerical stability condition and was about 0.8 μs for all numerical analysis conducted here.

3.2. *Modeling of Materials*

The stress and strain characteristic of concrete used for the finite element analysis are shown in Figure 5. For the compression region, assuming that concrete is yielded at 1,500μ strain, perfect elasto-plastic bilinear model was used. In this study, finally, yielding of concrete has been judged based on the Drucker–Prager's yield criterion. For the tension region, linear model was applied, but it is assumed that the stress cannot be transferred when a tensile pressure acted in the element reaches the breaking point. Here, the pressure is evaluated as an average of three normal stresses acted in each element and the tensile strength of concrete is assumed to be 1/10th of compressive strength similarly to the case of the numerical analysis for small-scale RC beams conducted by authors. Stress-strain relationship for main rebar and stirrup was defined using a bilinear isotropic hardening model. Plastic hardening coefficient H' was assumed to be 1% of Young's modulus E_s.

Yield of rebar and stirrup was calculated following von Mises yield criterion. Heavy weight, supporting gigues and anchor plates for axial rebars set at the both ends of RC girder were assumed to be elastic body because of no plastic deformation for those being found.

4. Analytical and Experimental Modeling Accuracy

In this study, numerical accuracies due to element size in the region near supporting gigue in the longitudinal direction, yield criterion for concrete material, system damping constant were investigated from the viewpoint of wave configuration of response. Numerical accuracies should be investigated for not only each parameter but also interaction between each two parameters considered here. However, those investigations need too much computation time. Then, here, the accuracy was investigated for each parameter considered here based on the finally determined input data by conducting preliminary analysis.

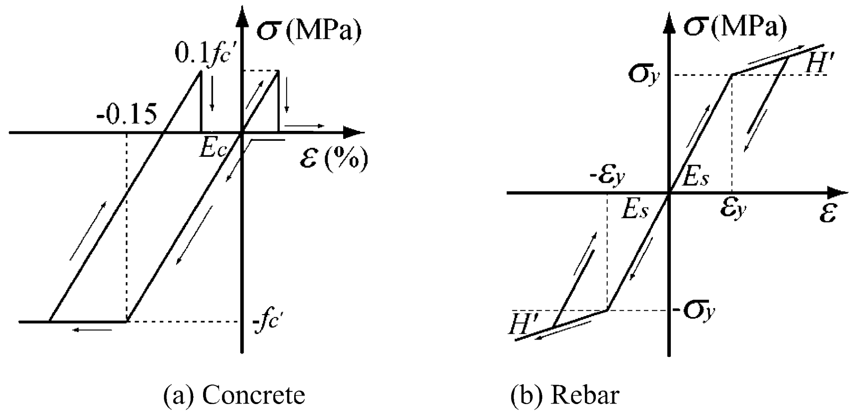

Fig. 5. Stress-strain relation of constitutive law model for materials.

Table 4. Analytical cases for investigating numerical accuracy by element size near support point.

Division near support point	Reinforced concrete modeling	Concrete yield criterion	Damping constant
4 Division 6 Division 8 Division	Beam element	Drucker–Prager	1.50%

4.1. *Element Size in Longitudinal Direction near Supporting Point*

Element size in the longitudinal direction near supporting point is basically set as one-half of an interval of stirrups and is 125 mm long. However, since an interaction between RC girder and the steel beam set on the upper surface of the girder for protecting jump up may influence to the numerical analysis on impact response behavior, numerical accuracy due to element size in the longitudinal direction was investigated, in which the element size in the region of 500 mm long back and forth of supporting point was considered. Here, three kinds of element size were taken as listed in Table 4, which are corresponding to those defined in the longitudinal direction of the RC girder, and element size for each four and eight division is the same for the elements near supporting part and the mid-span part, respectively, as shown in Figure 6.

Figure 7 shows the comparisons of analytical results for each response wave in case varying the mesh size of concrete elements near supporting point with the experimental results. From Figures 7(a) and 7(b), it is understood that the impact force wave at the beginning of impact can not be influenced by the element size near supporting point, but second dominant wave after 30 ms passed from the beginning of impact tends to be high amplitude with decreasing down of element size. From Figures 7(c) and 7(d), it is confirmed especially from Figure 7(d) that reaction force wave at the one supporting point tends to be high amplitude for high frequency component waves corresponding to element size decreasing and maximum amplitude in case of eight division was almost similar to that of the experimental results. From the comparison for displacement waves at the points $D - 1/2$ shown in Figures 7(e) and 7(f), it is observed that the wave during impact load surcharging behaves almost similar in spite of the element size near supporting point. Then, it is

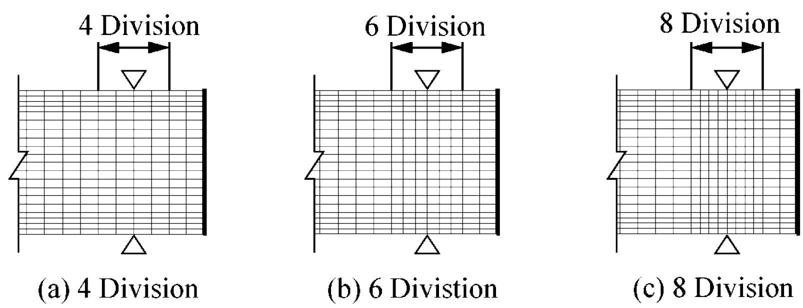

Fig. 6. FE division near 500 mm supporting point in longitudinal direction.

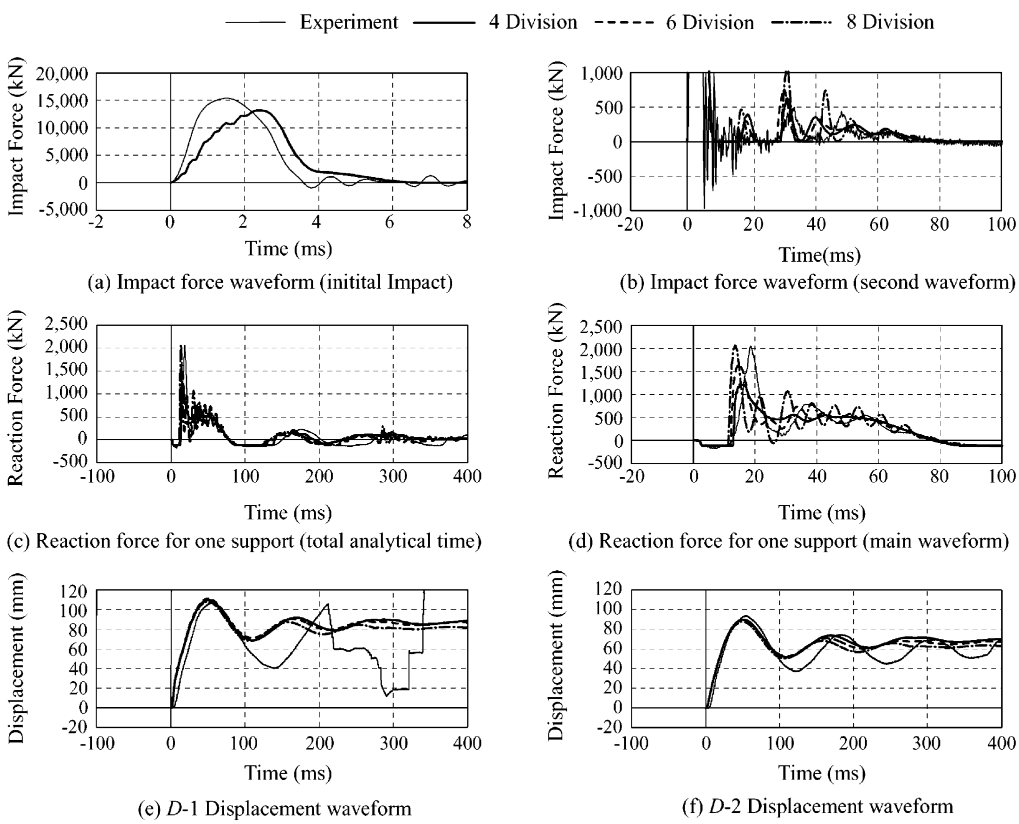

Fig. 7. Comparison of each response waveforms in case varying element size near support point.

confirmed from this investigation that the element size near supporting point will influence to the response of reaction force and maximum amplitude can be corresponded to the experimental results by dividing the 500 mm region near supporting point into eight elements in the longitudinal direction, in which the longitudinal length of those elements is the same to a quarter of an interval of stirrups.

Table 5. Analytical case for investigating numerical accuracy by yield criterion for concrete.

Concrete yield criterion	Division near support point	Reinforced concrete modeling	Damping constant
von Mises Drucker–Prager	8 Division	Beam element	1.50%

4.2. *Yield Criterion for Concrete Material*

In case analyzing concrete structure, since the confined effects of concrete material can be clearly appeared, it is generally pointed out that Drucker–Prager's yield criterion should be used. However, it has been seen by authors that elasto-plastic impact response behavior for small-scale RC beams under falling-weight impact loading can be better simulated using von Mises yield criterion (Kishi et al., 2005). In this study, an applicability of both yield criterion on impact response analysis for prototype RC girder was investigated with the parameters listed in Table 5 by comparing with the experimental results. The Drucker–Prager type yield criterion can be written as shown in Equation (1):

$$f(I_1, J_2) = \alpha I_1 + \sqrt{J_2} - k = 0, \tag{1}$$

where I_1 is the first invariant of stress tensor, J_2 is the second invariant of deviatoric stress tensor, α is a material constant, and k is a yield strength under pure shear. Coefficients α and k were determined referring to the book by Chen (1982) as $\alpha = 0.472$ and $k = 3.19$ MPa assuming that the tensile strength of concrete is 1/10th of compressive strength which is $f_t = 3.04$ MPa.

Figure 8 shows the comparisons of the impact response waves of the girder obtained using both yield criterion with the experimental results. From Figures 8(a) and 8(b), it is observed that time increment of the first dominant wave obtained using Drucker–Prager yield criterion is greater than that obtained using von Mises one. It is supposed that yield strength of concrete near impacted area is estimated so as to be upgraded due to three-dimensional confined effects in case using Drucker–Prager's yield criterion. However, even though Drucker–Prager's yield criterion is used, time increment of the wave cannot be increased up to that of the experimental results and the maximum amplitude is also a little smaller than experimental one.

From the comparisons of second dominant wave shown in Figure 8(b), it is observed that: (1) in case using von Mises yield criterion, impact force wave has not been excited during 65 ms after first dominant wave being excited, and then a half sine wave with high amplitude was excited. This wave configuration is greatly different from that of experimental results; and (2) on the other hand, in case using Drucker–Prager's yield criterion, four half-sine waves with a few ms duration time were excited with the time intervals of 10 to 15 ms and then the wave has been decreased to zero level. The wave configuration is some different from that of experimental results but is more similar to the experimental one than that obtained using von Mises yield criterion.

From Figure 8(c), it is seen that reaction force waves for one supporting point obtained using both yield criterion are almost the same to each other. The numerically estimated period for free vibration excited during a heavy weight being rebounded is shorter than that obtained from the experimental results in spite of yield criterion of concrete material. From Figure 8(d) of enlarged wave configuration in the beginning of impact, configurations of the first dominant wave obtained using both yield criterion are almost the same to each other. The maximum amplitude for those wave configurations is similar to that of experimental results but time increment of the wave at the

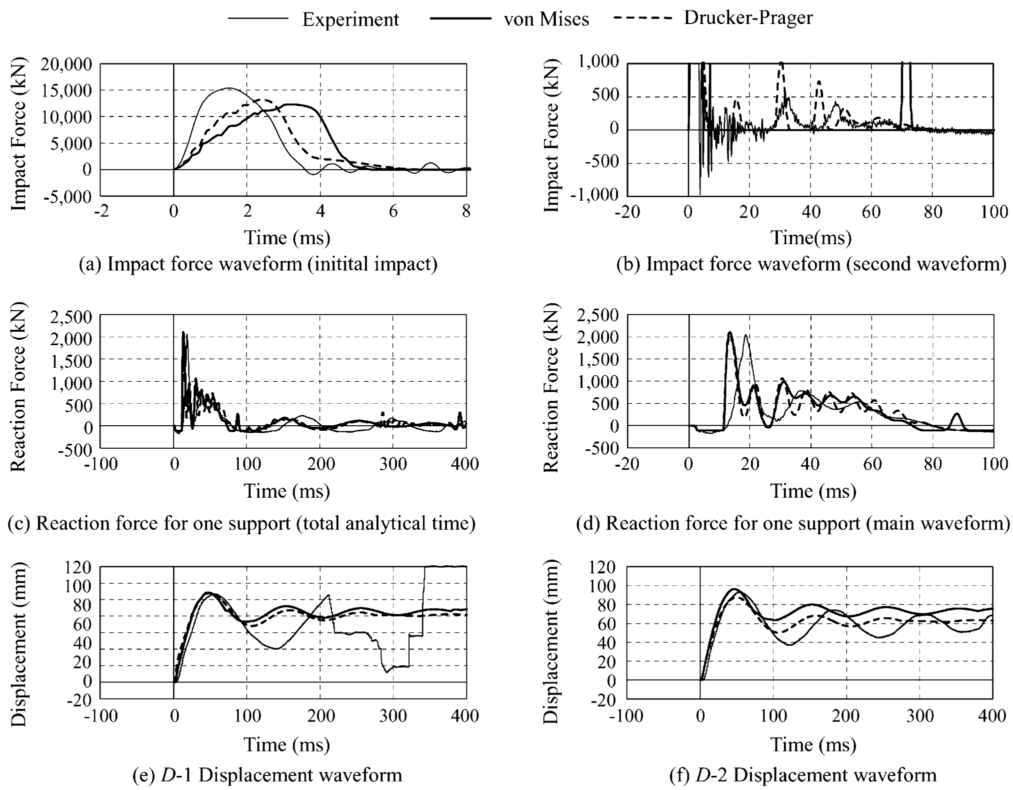

Fig. 8. Comparison of each response waveforms for changing yield criterion of concrete.

beginning of impact is larger than that of the experimental results and is contradictory to the case of impact force wave.

From Figures 8(e) and 8(f) for displacement waves at the points $D - 1/2$, it is confirmed that numerical response wave during the impact load surcharging to the RC girder is similar to that of the experimental results irrespective of yield criterion of concrete material considered here. From Figure 8(f), it is observed that numerically estimated period for free vibration during a heavy weight being rebounded is shorter than that from the experimental results as well as reaction force wave. Residual displacement obtained using Drucker–Prager yield criterion is almost the same to the experimental result but that obtained using von Mises yield criterion is estimated larger than the experimental result. This implies that the local stress concentration and confined effects of concrete near impacted area of the girder can be better evaluated by using Drucker–Prager's yield criterion. Then, in case of spherical head of a heavy weight impacting for the prototype RC girder, impact response behavior of the girder may be better analyzed using Drucker–Prager yield criterion for concrete material.

4.3. *Damping Constant h*

In the impact response analysis for prototype RC girders, system damping effects of the structure should be considered as well as the hysteretic damping effects of concrete and rebar material. Here, an appropriate viscous damping constant, h (hereinafter, damping constant) was determined with referring to the first natural vibration frequency. In this study, four cases were considered: $h =$

Table 6. In case of varying damping constant for concrete.

Damping constant	Division near support point	Reinforced concrete modeling	Concrete yield criterion
0.50% 1.00% 1.50% 2.00%	8 Division	Beam element	Drucker–Prager

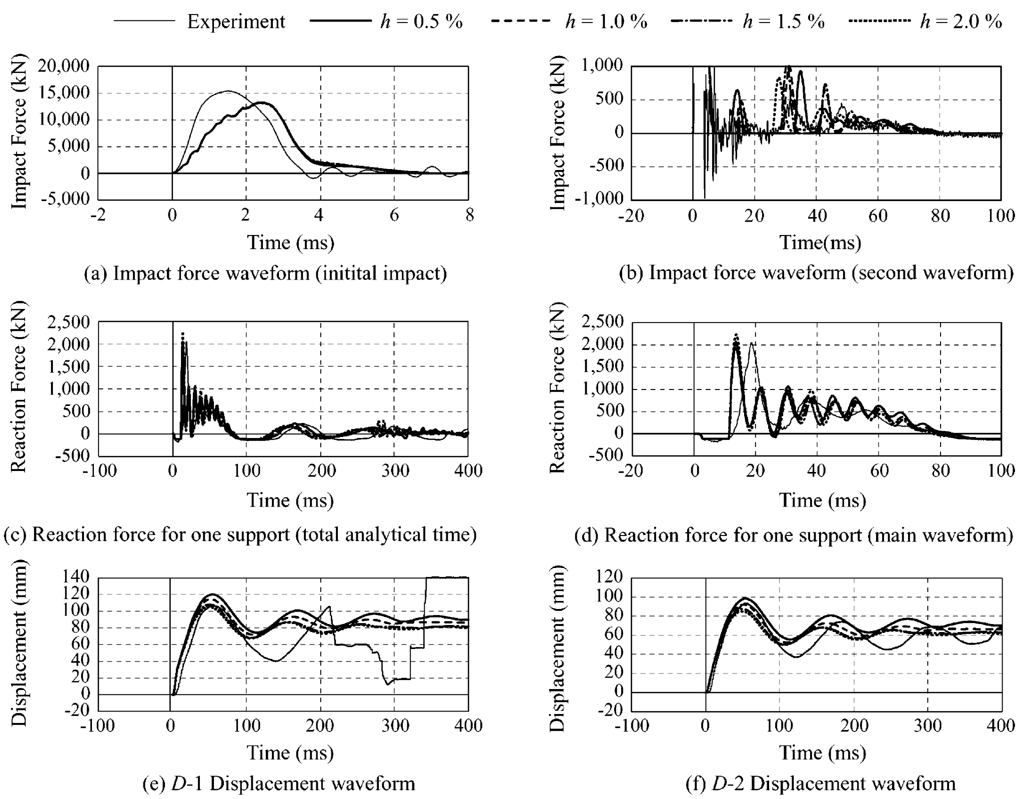

Fig. 9. Comparison of each response waveforms in case varying damping constant h.

0.005, 0.01, 0.015, and 0.02 with the design parameters as listed in Table 6. Figure 9 shows the comparison of impact response waves obtained varying damping constant h with those from the experimental results. From Figures 9(a) through 9(d), it is seen that: (1) maximum amplitudes of impact force and reaction force at one supporting point are hardly influenced by damping constant h; and (2) phase of the second dominant wave of impact force and reaction force wave during impact load surcharging tends to be large with increasing of damping constant h. From Figures 9(e) and 9(f) for the comparison of displacement waves at points $D - 1/2$, it is confirmed that maximum displacement and residual displacement tend to be large with decreasing of damping constant h and an appropriate damping constant may be $h = 0.015$.

5. Conclusions

To establish a simple elasto-plastic impact analysis method of flexure-failure-type RC girder, a falling-weight impact test and three-dimensional FE analyses were conducted for full-scale RC girder. The results obtained from this study are as follows:

(1) Changing yield criterion for concrete material from von Mises model to Drucker–Prager model, and applying system damping constant of $h = 0.015$, the maximum amplitudes and the configuration of primary wave for three waves: weight impact force; reaction force; and mid-span displacement, can be better simulated;
(2) To better simulate the characteristics of mid-span displacement wave, the region near supporting point should be modeled with fine mesh which is the same to a quarter of an interval of stirrups;
(3) Stress-strain relation of concrete assumed for analysis of small-scale RC beams can be applicable for the analysis of large-scale RC girders; and
(4) However, the initial gradient of weight impact force wave and frequency of secondary displacement wave cannot be properly estimated whatever any parameter is changed.

References

Chen, W.F., 1982, *Plasticity in Reinforced Concrete*, McGraw-Hill.
Hallquist, J.O., 2000, *LS-DYNA User's Manual*, Livermore Software Technology Corporation.
Japan Society of Civil Engineers, 1996, *Japan Concrete Standard*, JSCE [in Japanese].
Japan Society of Civil Engineers, 2004, *Practical Methods for Impact Tests and Analysis*, Structural Engineering Series 15, JSCE [in Japanese].
Kishi, N., Mikami, H., Matsuoka, K.G. and Ando, T., 1999, Elasto plastic impact behavior analysis of flexure failure type RC beam, *Journal of Structural Mechanics and Earthquake Engineering, JSCE*, 619(47), 215–233 [in Japanese].
Kishi, N., Nakano, O., Matsuoka, K.G. and Ando, T., 2001, Experimental study on ultimate strength of flexural-failure-type RC beams under impact loading, in *Transactions of the 16th International Conference on Structural Mechanics in Reactor Technology (SMIRT)*, Paper #1525.
Kishi, N., Mikami, H., Matsuoka, K.G. and Ando, T., 2002, Impact behavior of shear-failure-type RC beams without shear rebar, *International Journal of Impact Engineering*, 27, 955–968.
Kishi, N., Mikami. H, Namba. K. and Bhatti A.Q., 2005, Impact response analysis of light weight shear-failure type RC beams with stirrups, *Journal of Applied Mechanics JSCE*, 8, 471–480 [in Japanese].